Radial Profile and Confinement of Energetic Particles during NBI and ICRF Heating in LHD

S. Murakami 1), M. Osakabe 2), K. Ida 2), M. Yoshinuma 2), T. Ozaki 2), T. Tokuzawa 2), M. Isobe 2), M. Nishiura 2), P. Goncharov 2), E.A. Veshchev 2), Y. Takeiri 2), Y. Oka 2), K. Tsumori 2), K. Ikeda 2), K. Nagaoka 2), K. Saito 2), T. Seki 2), R. Kumazawa 2), H. Kasahara 2), T. Mutoh 2), O. Kaneko 2), A. Komori 2) and the LHD experimental group

1) *Department of Nuclear Engineering, Kyoto University, Kyoto 606-8501, Japan*
2) *National Institute for Fusion Science, Toki 509-5292, Japan*

e-mail address : murakami@nucleng.kyoto-u.ac.jp

Abstract. The energetic ion distributions and confinements are studied in the LHD plasma applying a newly developed radial profile measurement system FICXS (Fast Ion Charge Exchange Spectroscopy) based on the Doppler shifted Balmer-alpha (H_α) emission from the energetic ions charge-exchanged with injected neutral beams. A clear difference is found in the H_α emission spectrum changing the magnetic configurations from the neoclassical optimized (R_{ax}=3.53m) to the classical heliotron (R_{ax}>3.75m) configuration. The radial profiles of energetic ion distributions during ICRF heating are also investigated by the pellet charge exchange (PCX) measurement. These results are compared with the GNET simulations, in which the drift kinetic equation is solved in 5-D phase space, and show relatively good agreements.

1. Introduction

Because of the three dimensional magnetic configuration behaviours of trapped particles in a helical ripple are complicated. A good confinement of energetic particles is one of key issues in the development of a reactor based on a helical system. In LHD the neoclassical transport optimized configuration has been proposed by inwardly shifting the magnetic axis position, R_{ax}, from 3.75m to 3.53m[1]. In this case, the effective helical ripple is very small, remaining below 2% inside 4/5 of the plasma radius and the deviation of trapped particle orbit from magnetic surfaced is very small. Also Monte Carlo simulation results have also shown a good confinement of alpha-particle for a time longer than the energy slow-down time in the reactor scaled device[2]. Thus LHD is the first large size helical device in which the energetic ion confinement can be investigated in the both of the classical (R_{ax}>3.75m) and advanced stellarator (R_{ax}=3.53m) configurations.

The several energetic ion measurement systems based on the neutral particle analyzer (NPA) have been installed and the energetic ion distributions have been investigated in the NBI and/or ICRF heating plasmas in LHD[3-6]. Also the comparisons with the simulation results have been done and relatively good agreements are obtained[2,7]. However, the measured information by the NPA systems is obtained as an integrated value along a line of sight and the radial profile information is dropped, which is very important for the detail confinement analysis. Thus, a radial profile measurement system is necessary for the energetic ion confinement analysis.

In this paper we study the energetic ion distribution and confinements during NBI heating in the LHD plasma applying a newly developed radial profile measurement system, FICXS (Fast Ion Charge Exchange Spectroscopy)[8]. FICXS is based on the Doppler shifted Balmer-alpha (H_α) emission from the energetic ions charge-exchanged with injected neutral beams. The method is similar to the Fast Ion Deuterium-Alpha (FIDA) measurement [9,10]. The main difference is the geometry of NBI and the measured ion species. The results are compared with the GNET simulations, in which the drift kinetic equation is solved in 5-D phase space[2,7,12].

The energetic ion distributions during ICRF heating are also studied by PCX (Pellet Charge eXchange) measurement[11]. In the ICRF heating energetic ions more than 100keV is generated and it is very difficult to observe such high energy by the present FICXS measurement. The impurity pellet (poly-styrene) is injected to plasma and the charge-exchanged neutral particle between the pellet ablation cloud and energetic ion is observed from backward of the pellet trajectory. The results are compared with the GNET simulation.

In section 2 we will briefly explain the FICXS measurement system and the experimental results are shown. Then the comparisons of the energetic ion distribution with the GNET simulation results are shown. In section 3 we will show the results of PCX during the ICRF heating and the results are compared with the GNET simulation results. Finally, we conclude in section 4.

2. Radial Profile Analysis of Energetic Ions during NBI heating

2.1. FICXS Measurement System

The charge-exchanged energetic ion with the injected neutral beams emits the Doppler shifted Balmer-alpha (H_α). We can analyze the radial profile of energetic ion distributions by measuring this H_α light. We set up the H_α measurement system to see perpendicularly to the injected neutral beams by NBI (perpendicular injection, E_b<40keV). The edge neutral radiates brightly near the un-shifted wavelength (~656nm) of H_α line. The H_α emission from energetic ions is Doppler shifted away from these bright interfering signals.

Figure 1 shows the schematic view of the FICXS measurement system. The optics normally used for bulk ion temperature and poloidal flow measurements are utilized for the FICXS measurement. Two curved mirrors are installed in one toroidal section of LHD and light is reflected at these mirrors to 48 optical fibers so as to have a better spatial resolution of active CXS measurement with the radial-NBI. The same set of the measurement system is installed at a different toroidal location with the same plasma cross section for the measurement of background, where no interference by both of the tangential and perpendicular injection NBIs are expected.

2.2. Experimental results

The perpendicular injection NBI is applied in addition to the tangential injection NBI. We obtain the quasi-steady state plasma and measure the radial distribution of energetic ions by FICXS. Figure 2 shows the H_α emissions as a function of the wave-length changing the observing radial positions, r/a, in the R_{ax}=3.53m configuration. The electron temperature is about 2keV. The electron density is $n_e \sim 1.0\times10^{19} m^{-3}$.

We can see the increase of the intensity as the wavelength goes up in the region r/a<0.8. (Peaks near 649nm, 651nm and 652nm are due to the impurity line; shaded region.) This indicates the slowing down distribution of beam ions and no qualitative difference can be seen in the radial positions. The quantitative difference is mainly due to the damping of the neutral beam and the slowing down time.

Near the X-point we can see the clear peak positions (E0, E0/2, E0/3). These peaked intensity profiles agree well with the simulation assuming the charge exchange with the background thermal neutral. Therefore, we can confirm the measurement system about the Doppler shifted wavelength in these peak positions.

In order to separate the beam emission signals from the emission of impurity ions we change the injection energy from 28keV to 37keV and check the shift of the emission wavelength. Figure 3 shows the H_α emissions as a function of the wavelength changing the injection energy; (a) near the X-point and (b) r/a~0.6. We can see the shift of three peak positions as the injection energy increased from 28keV to 37keV. We also find the shift of the slowing down distribution of energetic ions near r/a~0.6. These indicate that the signals are actually emitted from the energetic hydrogen ions.

Next we study the configuration dependency of the energetic ion confinement comparing the results in the R_{ax}=3.53m through 3.9m configurations. We compare the plasma where the plasma density n_e~1.0x10^{19}m^{-3} and the temperature T_e~2keV. Figure 5 shows the configuration dependence in the different radial positions. We can see the no clear difference in the r/a=0.6 case where the deeply trapped particles are well confined even in R_{ax}=3.75m configuration. On the other hand we can see a clear reduction in the R_{ax}=3.90m results and in the R_{ax}=3.75m results (the region lower than 652nm). These indicate the ripple transport of beam ions becomes large at plasma edge region in these configurations. We also found that the radial profile of the beam ions strongly depend on R_{ax}.

2.2 Comparisons with GNET Simulation Results

In order to make clear the configuration difference in the energetic particle confinement we compare the experimental results with GNET simulation results. In this code the drift kinetic equation for the energetic particle is solved in 5-D phase space and the global distributions of energetic ions can be accurately evaluated.

We solve the drift kinetic equation for NBI injected beam ions in 5D phase-space

$$\frac{\partial f}{\partial t} + (\mathbf{v}_{//} + \mathbf{v}_D)\cdot\nabla f + \mathbf{a}\cdot\nabla_{\mathbf{v}} f = C(f) + S_{beam} + L_{particle} \quad (1)$$

where *C(f)* are the linear Clulomb Collision operator. S_{beam} is the NBI beam ion source calculated by HFREYA code[8]. $L_{particle}$ is the particle sink (loss) term consists of two parts; one is the loss by the charge exchange loss assuming the same neutral particle profile as the source term calculation and the other is the loss by the orbit loss escaping outside of outermost flux surface. In GNET code the beam ion distribution *f* is evaluated through a convolution of S_{beam} with a characteristic time dependent Green function evaluated using test particle Monte Carlo method.

We evaluated the beam ion distributions by the perpendicular injection NBI in 5-D phase space assuming the similar temperature and density plasma. Figure 5 shows the obtained beam ion distribution for two different radial positions r/a=0.6 and 0.8; R_{ax} =3.53m (top), R_{ax} =3.75m (center) and R_{ax} =3.9m (bottom). The distributions are plotted in the velocity space and normalized with the thermal velocity of plasma at the center.

In the R_{ax}=3.53m case we can see the slowing down distribution of perpendicularly injected beam ions ($v_0/v_{th} \approx 5$). Comparing the R_{ax}=3.53m and R_{ax}=3.75m results we can see a similar tendency in the region $v_0/v_{th} \geq 3$ in the r/a=0.6 but the distribution is decreased in the region $v_0/v_{th} \leq 3$because of the radial diffusion by the pitch angle scattering. In the r/a=0.8 we can see the actual decrease of distribution in the R_{ax}=3.75m case. In the R_{ax}=3.9m case we can see a clear loss of energetic ions during slowing down and the distribution disappear in the region $v_0/v_{th} \leq 3$.

Using the obtained beam ion distribution we simulate the H_α emission and evaluate the intensity of FICXS signals. Figure 6 shows comparisons of the simulated H_α emission intensity of FICXS measurement with that of experimental ones for two different radial positions, r/a=0.6 and 0.8 and three configurations. In the r/a=0.6 the reduction of the intensity only in the R_{ax}=3.9m case and the small reduction of the intensity in the higher wavelength region in the r/a=0.8 in the R_{ax}=3.75m case.

As a result, we obtain relatively good agreement between the experimental and GNET simulation results. This indicates that the energetic ion distribution is well described by the model using in the GNET.

3. Radial Profile Analysis Energetic Ions during ICRF heating

We study the radial profile of energetic ion distribution applying 2^{nd} harmonics ICRF heating to the NBI heated plasma. In the 2^{nd} harmonics heating the energetic ions injected by NBI mainly interact with ICRF waves. Therefore the behaviour of beam ion plays an important role in the 2^{nd} harmonics ICRF heating.

The radial profile of the energetic ion distribution is observed by the pellet charge exchange neutral particle measurement (PCX). We inject an impurity pellet (poly-styrene) and detect the charge-exchanged neutral particle between the pellet ablation cloud and the energetic ion. Thus we can translate the time trace of the energy spectrum to the radial profile by monitoring the accurate pellet velocity.

The 2^{nd} harmonic ICRF power (38.47Mhz) is launched to the plasma (hydrogen) sustained by the tangentially injected NBI and the perpendicular injection NBI is added. The magnetic strength on axis is 1.375 T. The innermost normalized minor radius of the resonance layers was 0.5. Figure 7 shows the radial profile of the energetic ions spectrum obtained from the time resolved energy spectrum. The beam ions are accelerated by ICRF waves to higher energy perpendicularly. The enhancement of energetic ion distribution is observed near the ICRF resonance region (r/a=0.5) by the PCX measurements.

We evaluated the energetic ion distributions by the ICRF heating in 5-D phase space assuming the similar temperature and density plasma. The ICRF heating term is introduced in Eq. (1) in the ICRF heating calculation by GNET. In the simulation the tangentially and perpendicularly injected NBI beam ions are calculated interacting with the ICRF waves. Figure 8 shows the obtained energetic ion distribution during ICRF heating; (a) in the velocity space and (b) in the r/a-energy space. We can see the acceleration to the perpendicular direction both of tangential and perpendicular injected NBI beam ions (two peaks in the perpendicular velocity direction). We can see a relatively good agreement in the radial and energy distribution with the experimental ones in the Fig. 8-(b).

4. Conclusions

We have studied the energetic ion distributions and confinements during NBI heating in the LHD plasma (classical to advanced stellarator configurations) applying a newly developed radial profile measurement system FICXS based on the Doppler shifted Balmer-alpha (Hα) emission from the charge-exchanged energetic ions. A clear difference has been found in the H_α emission spectrum depending on the configurations. We have also studied the energetic ion distribution and confinement during ICRF heating applying PCX measurement. These results are compared with the GNET simulations and show relatively good agreements.

These facts indicate that the ripple transport (neoclassical processes) dominates the energetic ion confinement and make sure the numerical prediction of the energetic ion confinement in helical reactor studies.

References

[1] S. Murakami, et al.," The Neoclassical-Transport-Optimized Configuration of the LHD", Nucl. Fusion 42 (2002) L19.
[2] S. Murakami, et al., "Effect of Neoclassical Transport Optimization on Energetic Ion Confinement in LHD", Fusion Sci. Technol. 46 (2004) 241.
[3] M. Isobe, et al., "Charge exchange neutral particle analysis with natural diamond detectors on LHD heliotron", Rev. Sci. Instrum. 72, 611 (2001)
[4] A.V. Krasilnikov, et al., "Study of acceleration and confinement of high-energy protons during ICRF and NBI heating in LHD using a natural diamond detector", Nucl. Fusion 42, 759 (2002).
[5] T. Ozaki, et al., "High-energy neutral particle measurement system in the large helical device", Rev. Sci. Instrum. 71, 2698 (2000)
[6] M. Osakabe, et al, "Evaluation of energetic particle confinement using CXNPA with NB-blip experiments on Large Helical Device", Rev. Sci. Instrum. 75 3601
[7] S. Murakami, et al., "A global simulation study of ICRF heating in the LHD", Nucl. Fusion 46 (2006) S425-S432.
[8] M. Osakabe, et al., "Fast ion charge exchange spectroscopy measurement using a radially injected neutral beam on the Large Helical Device", Rev. Sci. Instrum, 2008 in press.
[9] W.W. Heidbrink, et al., "Hydrogenic fast-ion diagnostic using Balmer-alpha light", Plasma Phys. Control. Fusion 46 (2004) 1855.
[10] W.W. Heidbrink, et al., "Fast-ion D-alpha diagnostic for NSTX", Rev. Sci. Instrum. 77, 10F120 (2006).
[11] T. Ozaki, et al., "Horizontal, vertical, and radial high-energy particle distribution measurement system in Large Helical Device", Rev. Sci. Instrum. 77, 10E917 (2006).
[12] S. Murakami, et al., "5D Simulation Study of Suprathermal Electron Transport in Non-Axisymmetric Plasmas", Nucl. Fusion 40 (2000) 693.

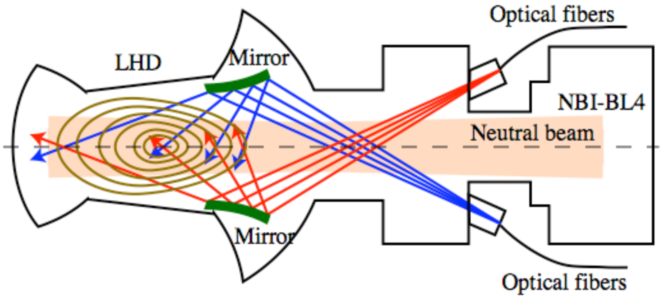

FIG. 1. Schematic view of the FICXS measurement.

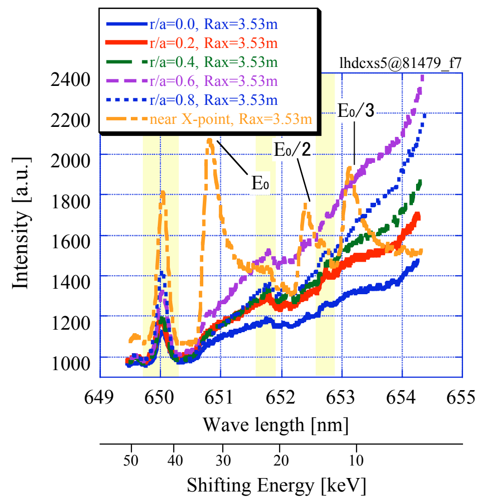

FIG. 2. H_α emissions as a function of the wavelength changing the observing radial position, r/a, in the Rax=3.53m configuration. (Peaks near 649nm, 651nm and 652nm are due to the impurity line)

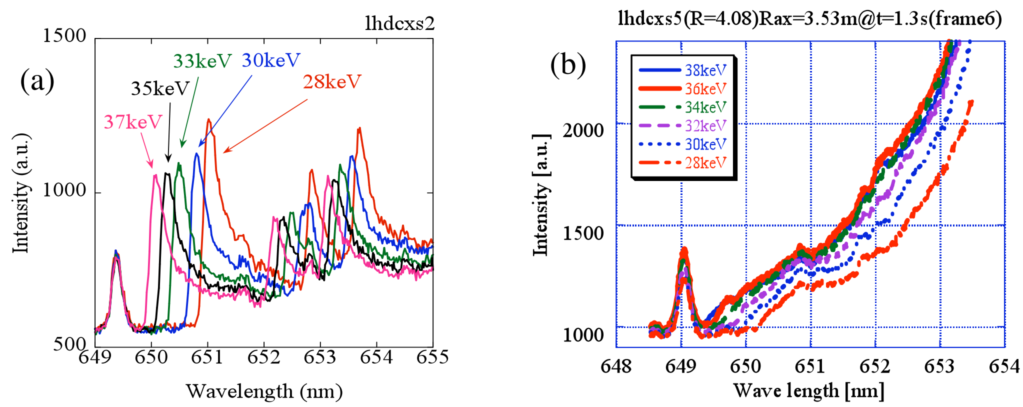

FIG. 3. H_α emissions as a function of the wavelength changing the NBI injection energy from 28keV to 37keV: (a) near the X-point and (b) near r/a=0.6.

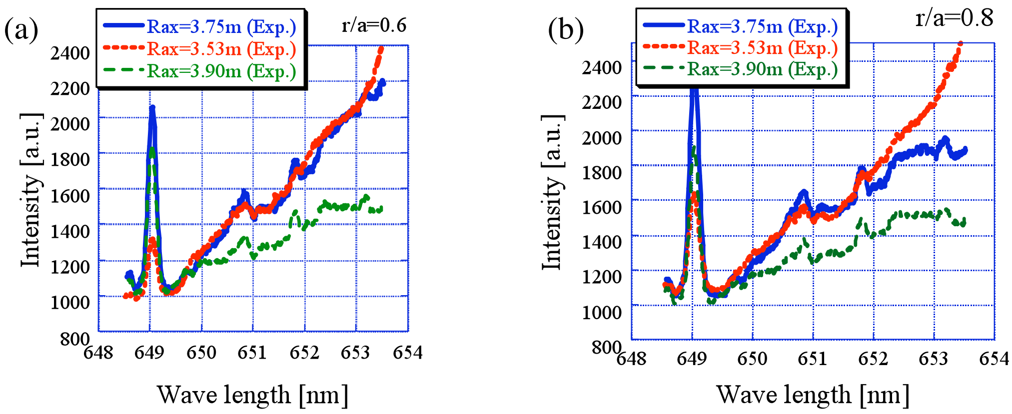

FIG. 4. H_α emissions as a function of the wavelength changing the magnetic configuration by the shift of the magnetic axis position from 3.53m to 3.9m; (a) r/a~0.6 and (b) r/a~0.8.

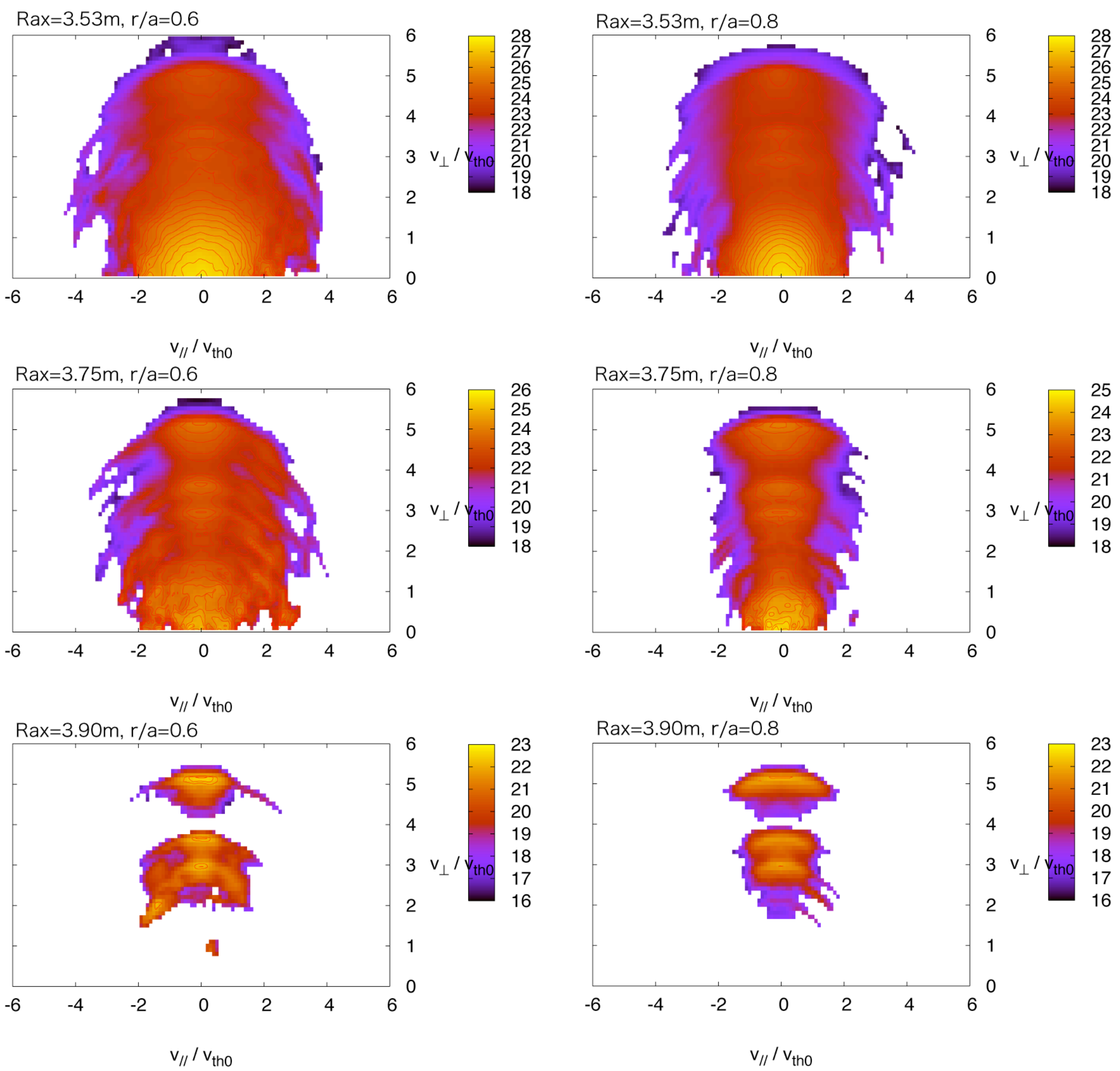

FIG. 5. Beam ion distribution of Perpendicular injection NBI in the (r/a, v_perp, v_para) space evaluated by GNET simulation.

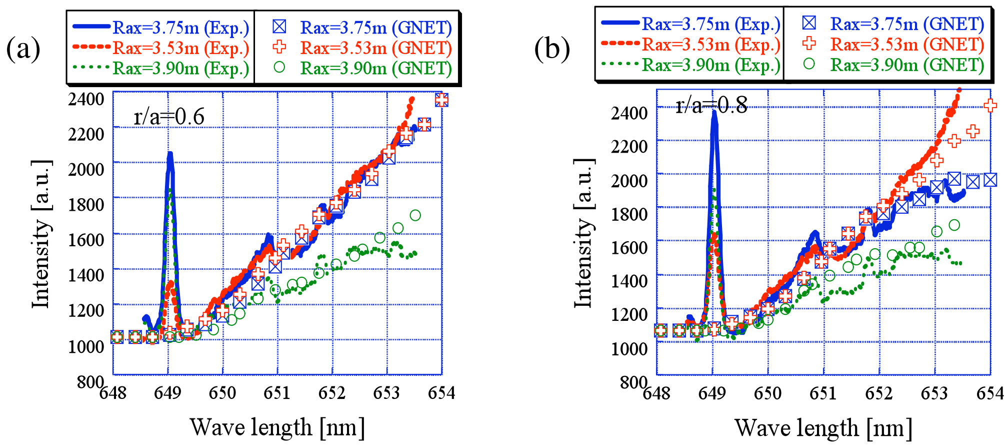

FIG. 6. Comparisons of the FICXS measurement results with the simulated one by GNET. (a) r/a~0.6 and (b) r/a~0.8.

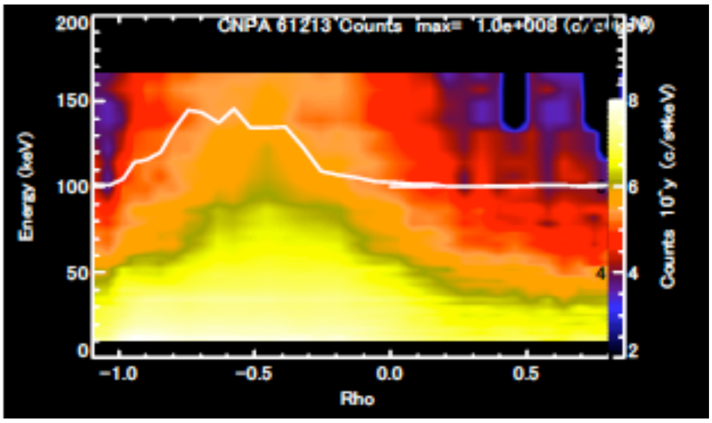

FIG. 7. Radial distribution of energetic ions during ICRF heating in LHD.

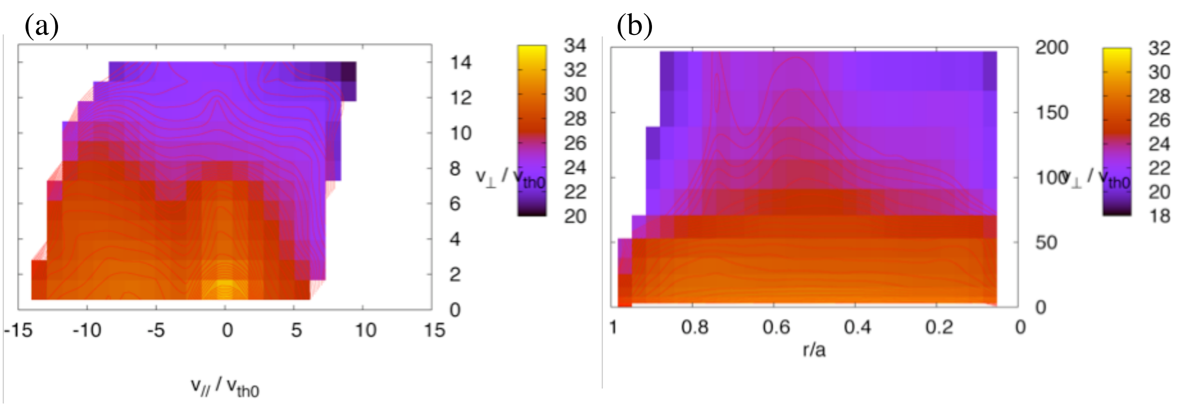

FIG. 8. Energetic ion distribution obtained during ICRF heating by GNET simulation in LHD; (a) in the velocity space and (b) in the r/a-energy space.